LANGMUIR

pubs.acs.org/Langmuir Article

Polymer Free Volume Effects on Protein Dynamics in Polystyrene Revealed by Single-Molecule Spectroscopy

Nicholas A. Moringo,[#] Hao Shen,[#] Lawrence J. Tauzin, Wenxiao Wang, and Christy F. Landes*

Cite This: *Langmuir* 2020, 36, 2330−2338 Read Online

ACCESS | Metrics & More | Article Recommendations | Supporting Information

ABSTRACT: Protein−polymer interactions are critical to applications ranging from biomedical devices to chromatographic separations. The mechanistic relationship between the microstructure of polymer chains and protein interactions is challenging to quantify and not well studied. Here, single-molecule microscopy is used to compare the dynamics of two model proteins, α-lactalbumin and lysozyme, at the interface of uncharged polystyrene with varied molecular weights. The two proteins exhibit different surface interaction mechanisms despite having a similar size and structure. α-Lactalbumin exhibits interfacial adsorption−desorption with residence times that depend on polymer molecular weight. Lysozyme undergoes a continuous time random walk at the polystyrene surface with residence times that also depend on the molecular weight of polystyrene. Single-molecule observables suggest that the hindered continuous time random walk dynamics displayed by lysozyme are determined by the polystyrene free volume, a finding supported by thermal annealing and solvent quality studies. Hindered dynamics are dominated by short-range hydrophobic interactions where the contributions of electrostatic forces are negligible. This work establishes a relationship between the microscale structure (i.e., free volume) of polystyrene polymer chains to nanoscale interfacial protein dynamics.

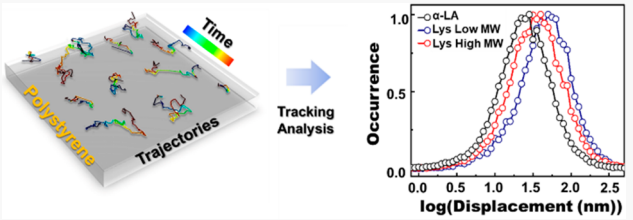

INTRODUCTION

Advancing the understanding of structure−function relationships in protein−polymer interactions is critical in the design of biosensing devices,[1,2] biocompatible implants,[3,4] and protein separations.[5−7] The adsorption of proteins to a polymer alters the material's function because the outermost layer of the material is comprised of proteins.[4] Polymers often experience protein accumulation when exposed to protein-rich environments, which has been shown to cause harmful side effects for patients[8,9] or reduced functionality in everyday health care products, such as contact lenses.[10,11] Surface modifications such as ligand grafting and UV exposure are used to suppress protein adsorption while keeping the bulk polymer properties unchanged.[12−14] Polymer chain architecture and packing densities are also used to modify polymer surface chemistries to reduce protein interactions,[15−17] but further work is needed to understand and control the underlying polymer chemistry and physics that control protein surface interactions.

Polymer free volumes are the naturally occurring voids that are present in a polymer material and depend on polymer chemistry and deposition conditions. The free volume of a polymer can have a dramatic effect on many physical characteristics such as the glass transition temperature,[18,19] diffusivity in the polymer matrix,[20,21] and the aging process.[22] Polymer free volume can be altered by mechanically compressing the polymer, thermally annealing,[23] and changing the molecular weight (MW) (i.e., chain length) of the polymer used to develop a film.[18] It has also been shown that using poor solvents with low solubility to dissolve polymers before deposition or spin-casting can influence the free volume in bulk polymers.[18] However, there is little knowledge about how polymer free volumes affect protein dynamics at polymer interfaces. Understanding the relation between microscale polymer packing and protein behavior at polymer films could be invaluable in guiding the fabrication of improved materials.

Quantifying nanoscale protein dynamics at the surface of polymers is experimentally challenging. Many common techniques suffer from ensemble averaging[24,25] or require *ex situ* sample conditions to measure.[26,27] Single-molecule fluorescence spectroscopy is a robust method for studying protein−polymer interactions allowing for many proteins to be tracked in real time below the diffraction limit of light.[28−30] For example, Schwartz et al. showed how poly(ethylene glycol) (PEG) brush grafting decreased fibronectin adsorption, but longer PEG chains led to more unfolding and longer residence times for adsorbed fibronectin.[31] Other single-molecule studies have established relationships between the microstructures of polymer brushes[13,32,33] and self-assembled monolayers[34,35]

Received: November 13, 2019
Revised: February 19, 2020
Published: February 20, 2020

https://dx.doi.org/10.1021/acs.langmuir.9b03535
Langmuir 2020, 36, 2330−2338

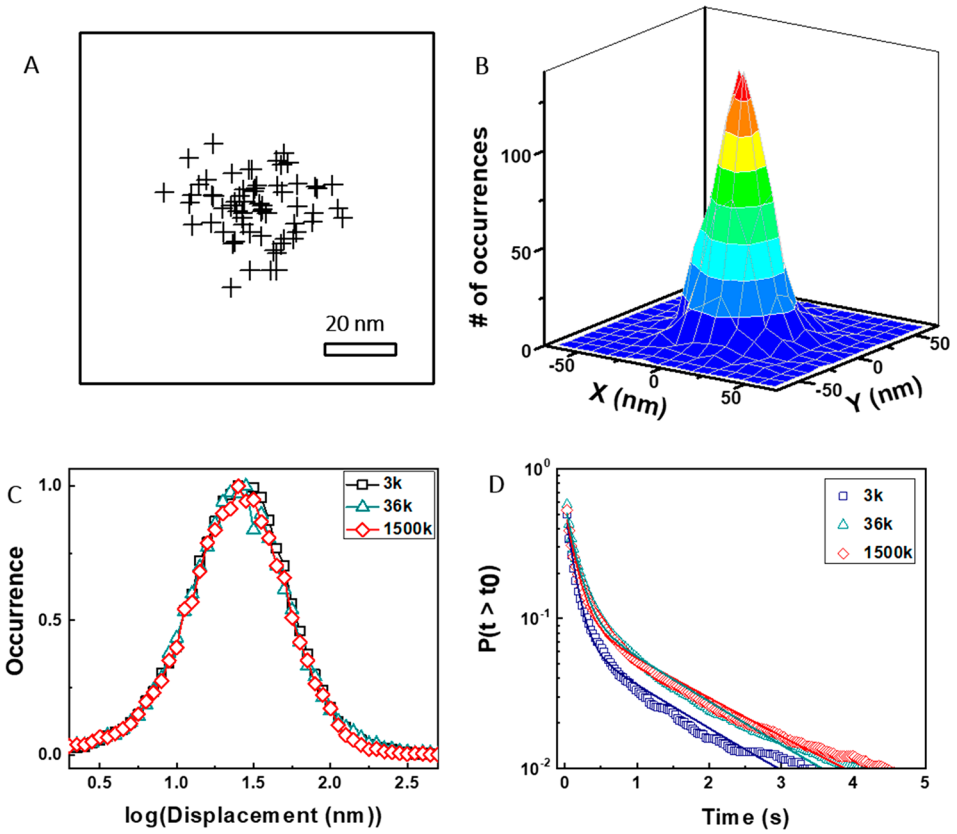

Figure 1. α-LA adsorption and dynamics at PS films. (A) The central localization for a single α-LA in 63 consecutive frames. (B) 2D histogram of combined central localizations from 20 α-LA molecules. (C) Single-frame displacement distributions for α-LA adsorbed onto PS films with varied PS MWs. (D) α-LA surface residence time cumulative distributions fits to eq 1 (solid lines).

with molecular probes, but a relationship between thin film polymer packing and protein dynamics is lacking. Using total internal reflectance geometry[36−38] achieves increased signal-to-noise by suppressing emission from molecules diffusing in the bulk. The utility of single-molecule fluorescence microscopy also has broader application to nanoparticle catalysis,[39] live-cell imaging,[40] and improving chromatographic separations.[41−43]

In this study, we compare the surface dynamics of two oppositely charged proteins, lysozyme (Lys, positive)[44] and α-lactalbumin (α-LA, negative),[45] at thin uncharged polystyrene (PS)[46] films with varied free volumes. Lys and α-LA are of interest given their common use as model proteins[47−51] and due to their similarities in size and structure.[52,53] PS is chosen because the variation in PS free volume is well studied[18,47,48] and because of its use in common applications.[54−56] Lys and α-LA are found to exhibit different types of motions at PS surfaces. α-LA undergoes single-site adsorption−desorption at PS, with a MW dependence on surface residence times. Lys undergoes non-Brownian surface transport known as a continuous time random walk (CTRW), where adsorption occurs at nonspecific sites for random periods of time interrupted by desorption to nearby sites.[17,57,58] The Lys CTRW dynamics depend on the MW of the PS film, with fewer hops and smaller hop sizes at higher MWs. We propose the observed MW dependence on Lys dynamics is caused by the free volumes among PS chains in the deposited films.[18] This interpretation is supported by thermal annealing studies as well as changing solvent quality. Lastly, PS is doped with a hydrophilic polymer (methoxypolyethylene glycol) to determine that short-range hydrophobic interactions dominate the hindered Lys dynamics on PS with varied free volumes.[59] Further, tracking results under varied ionic conditions suggest that electrostatic forces do not contribute to varied Lys dyanmics at PS. We envision that this single-molecule approach can be widely applied for the observation of many protein surface interactions to develop more robust materials for specific applications in protein-rich environments.

MATERIALS AND METHODS

Preparation of Polymer Films. Borosilicate glass coverslips (22 × 22 mm, VWR) were thoroughly cleaned by sequentially sonicating in water, ethanol, and acetone. The coverslips were then placed in a piranha bath (28% NH_4OH and 30% H_2O_2) heated at 80 °C for 20 min. After they were rinsed with deionized water (>1 MΩ·cm) and dried with N_2 gas (Ultrapure, Airgas), the coverslips were further treated with oxygen plasma (Harrick Plasma, PDC-32G) for 2 min. Thin PS films were prepared by spin-coating (SPI KW-4A) a 1 w/w% PS/toluene or PS/cyclohexane solution at 3000 rpm for 1 min. PS of various MWs of 3k (Polymer Source, PDI: 1.09), 36k (Polymer Source, PDI: 1.05), and 1500k (Polymer Source, PDI: 1.10) were prepared using the spin-coating protocol. The surface roughness of resulting films was measured by atomic force microscopy (Bruker, Multimode 8) operated in peak force tapping mode.

Polymer Film Thickness and Refractive Index Characterization. For all molecular weights (3k, 36k, and 1500k), annealed PS and solvent adjusted film solutions of 1 w/w% PS/toluene or cyclohexane were coated (100 μL) at 3000 rpm for 1 min onto cleaned silicon wafers (Silicon Quest Int'l, Prime grade) with a spin coater (Laurell WS-650MZ-23NPPB). Resulting film thicknesses and refractive indices were measured with a J.A. Woollam M-2000 ellipsometer scanning from 350 to 1050 nm. Data were fit with the

https://dx.doi.org/10.1021/acs.langmuir.9b03535
Langmuir 2020, 36, 2330−2338

Cauchy thin film model resulting in a mean squared error of less than 5% for all measurements, and the results are presented in Table S1.

Film Annealing and Modification. A hot plate was placed inside a glovebag filled with N_2 gas (Ultrapure, Airgas). After the PS samples were placed on the hot plate, the temperature was elevated to 120 °C for 4 h. Once finished, the PS samples were cooled to room temperature under an N_2 atmosphere.

mPEG Doping of PS. The hydrophilic films were prepared by spin coating clean coverslips with 1 w/w% toluene solution containing PS and methoxypolyethylene glycol (mPEG) with a weight ratio of 9:1, using the same conditions described above for the pure PS samples. AFM imaging (Bruker, Multimode 8) of mPEG/PS films was performed in tapping mode to acquire phase images for determining the spatial surface coverage of mPEG domains (Figure S1). Results indicate that the mPEG domains are highly uniform in the mPEG/PS films.

Protein Dilutions and Fluorescence Labeling. Lyophilized lysozyme (pI = 10.7)[44,60] labeled with rhodamine B (structure in Figure S2) was purchased from Nanocs as previously described.[17] Alexa 555 (structure in Figure S2) labeled α-LA (pI = 4.2),[45,61] previously purified and acquired from the Wilson Group at the University of Houston, was used here.[36] For experiments, α-LA and Lys were diluted in 10 mM HEPES buffer (pH = 7.2) to form 3.5 and 35 nM solutions, respectively.

Protein Surface Charge and Hydrodynamic Measurements. A Malvern zetasizer (Zen 3600 Nanoseries) was used to measure the zeta potentials and hydrodynamic radii of α-LA and Lys in 100 mM HEPES at pH 7.2. Zeta potential experiments were performed in Malvern cuvettes (DTS1070) with the average and standard deviation of 35 measurements reported. Hydrodynamic radii values from 13 measurements were quantified with the average and standard deviation. All measurements were taken at 25 °C after 2 min of equilibration.

Single-Molecule Measurements. A custom-built total internal reflection fluorescence (TIRF) microscope was used for single-molecule fluorescence measurements. A 532 nm laser (Coherent, Compass 315M-100SL) was circularly polarized and passed through a 100× oil-immersion objective (Carl Zeiss, Alpha Plan-Fluar, NA = 1.45) to excite the labeled proteins. The excitation light was focused on a 30 × 20 μm^2 area. The fluorescence signal from the proteins was collected by the same objective, filtered by two filters (Kaiser, HNPF-532.0−1.0 and Chroma, ET585/65m), and then collected by an electron-multiplying charged coupled device (Andor, iXon 897) cooled at −70 °C and operated at 33.33 Hz. The transmittance of PS is greater than 85%, with a refractive index of 1.58;[62] therefore, TIRF excitation takes place at the PS aqueous interface as previously shown (Figure S3).[17] The evanescent field in our TIRF geometry has a maximum penetration depth of 200 nm,[28] thus only fluorescent probes near the polymer surface are excited. Prior to measurements, the observation area was photobleached with laser excitation for 30 min to remove any fluorescent signal from contaminants present in the film. For single-molecule experiments, either α-LA or Lys solution (1 mL) was drop-cast onto the polymer film covering an area greater than the area illuminated by laser light.

Protein Molecule Identification and Tracking. An established tracking algorithm was used to identify and track both α-LA and Lys molecules.[63] This Matlab-based program has three fundamental steps for tracking single-molecules below the diffraction limit of light, i.e., increase the signal-to-noise, identify molecules, and utilize a nearest neighbor algorithm to generate single-molecule trajectories.[63] The Troika tracking program is available at https://github.com/LandesLab/Troika-Single-particle-tracking.

RESULTS AND DISCUSSION

α-LA Adsorption and Dynamics at PS Surface. Superlocalization imaging of α-LA adsorption events shows that α-LA undergoes interfacial adsorption/desorption at the PS surface, with a localization uncertainty of 20 nm (Figure 1).[28] Individually adsorbed negatively charged α-LA molecules ($\zeta = -18 \pm 7$ mV)[45] are observed at the PS surface once α-LA solution is added to the PS (Figure S3). Adsorption events appear to be stationary over multiple frames, and within our spatial resolution[43,64] before disappearance due to desorption,[28] suggesting that the α-LA molecules adsorb to nonspecific surface sites on the PS. For adsorption events lasting more than one frame, each corresponding point spread function is fit to a 2D Gaussian distribution in each individual frame to extract the central localizations (Figure 1A). To increase statistics, the central localizations from 20 different α-LA molecules are compiled by aligning their centers of mass (Figure 1B).[65,66] The resulting 2D histogram is further fit by another 2D Gaussian, resulting in a full-width at half-maximum of 20 nm. This value is equivalent to the resolution limit of other commonly known super-resolution techniques such as PALM,[67] STORM,[68] and mbPAINT,[69] suggesting that α-LA molecules are stationary at the PS surface. Single-molecule tracking also corroborates the superlocalization findings, which are discussed next.

Single-molecule tracking further confirms that α-LA molecules are stationary over multiple frames and within our resolution limit[43,64] upon adsorption at PS independent of MW. The MW of the PS films is varied from 3k up to 1500k to assess the role of varied PS free volume on the immobile α-LA molecules.[18] Single-frame displacement distributions allow for the frame-to-frame displacements to be quantified from single-molecule trajectories (Figure 1C). The distributions of single-frame displacements from hundreds of α-LA molecules result in one peak centered at 24 nm (antilog, $10^{1.38}$) which is independent of the PS MW (Figure 1C). It is expected that the interfacial chemical identities of all three MW PS films are similar given that the solvent, concentration, and spin-coating processes are identical for all three MWs. Peak values from single-frame distributions closely match our localization uncertainty results in Figure 1A−B and values reported in previous studies.[34]

α-LA surface residence times depend on the MW of the underlying PS, as shown in Figure 1D. The cumulative distributions of surface residence times for α-LA indicate that the time spent on the surface increases as the MW increases. Residence time distributions are fit to a two-term exponential (eq 1)[70] to extract desorption rate constants as a function of PS MW (Table S2).

$$P(t) = A_1 e^{-k_1 t} + A_2 e^{-k_2 t} \quad (1)$$

Two-term exponential decay fits to residence time distributions have been shown to resolve the kinetics of folded and unfolded proteins populations,[43] resolve DNA hybridization kinetics,[71] and quantify the desorption kinetics from weak and strong adsorption sites intrinsic on polymer surfaces.[64] It is likely that anomalously strong sites exist on the PS surface due to the chemical stability of the globular proteins used here.[72] Decreased desorption rate constants observed at higher MWs suggest that longer PS chains induce stronger α-LA-PS interactions, thereby increasing the prevalence of long-lived adsorption events (Figure 1D). It has been shown that PS chains are more densely packed and more coiled as the MW of PS is increased in a deposited PS film (Table S1).[73] Therefore, we predict the number of short-range interactions (i.e., van der Waals, hydrogen bonding, and hydrophobic interactions) present between α-LA and PS increases in the more coiled PS at higher MWs. This hypothesis is supported by the findings of Schwartz and co-workers, which suggest that the

https://dx.doi.org/10.1021/acs.langmuir.9b03535
Langmuir 2020, 36, 2330−2338

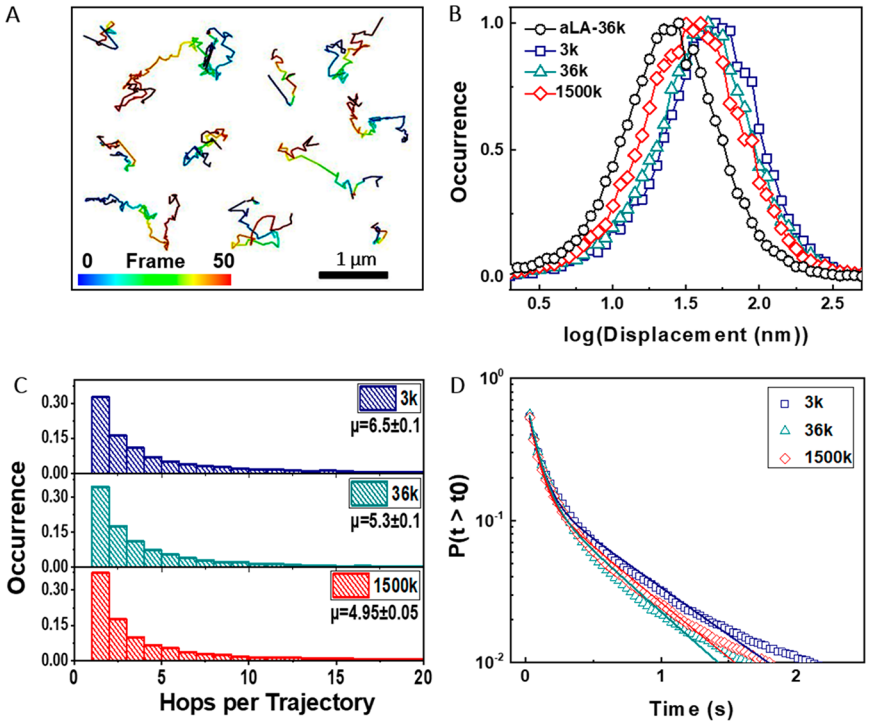

Figure 2. Lys adsorption and dynamics at PS films. (A) Representative trajectories of single Lys at the interface of PS (MW = 36k) with the color map representing the frame number for each trajectory. (B) Single-frame displacement distributions for Lys on PS films with varied MWs. α-LA distribution shown for comparison. (C) Lys hopping distributions with the calculated mean and standard error of the mean at each MW of PS. (D) Cumulative distribution of surface residence time for Lys with fits to eq 1 shown in the solid lines.

desorption of proteins from interfaces is dictated by short-range interactions rather than long-range interactions.[59] Therefore, tracking results indicate that desorption kinetics of α-LA are related to interactions with the underlying microscale organization of PS chains.

Lys Adsorption and Dynamics at PS Surface. Lys dynamics at PS are non-Brownian and exhibit CTRW behavior,[74] with surface transport dynamics that are dependent on the MW of PS. This result is surprising given the similarity in sizes (R_h = 1.6 ± 0.3 nm and R_h = 1.5 ± 0.2 nm for Lys and α-LA, respectively),[60,61] structures,[52,53] and biological ancestries[75−77] of Lys and α-LA (Figure S4). Representative trajectories are shown in Figure 2A to illustrate the CTRW motion of the positively charged Lys (ζ = 12 ± 6 mV)[44] at PS. The trajectories highlight the heterogeneity exhibited by individual Lys molecules at PS. Large areas of the PS surface are explored with brief periods of immobility at nonspecific adsorption sites as is typical of CTRW dynamics. The difference in Lys and α-LA dynamics is likely driven by the decreased affinity Lys exhibits for the PS surface, allowing Lys to explore the PS surface. A 10-fold higher concentration of Lys is needed to acquire similar surface coverage observed for α-LA at PS. The difference in adsorption strengths of α-LA and Lys are not attributed to the different dye labels used here (Figure S5). The CTRW mechanism of proteins at polymers has been observed by others at the single-molecule level.[47] Lys waiting time distributions, the time spent at each adsorption site, are analyzed and fit to a power law to verify the presence of the CTRW mechanism (Figure S6).[78] Waiting time distributions would be normally distributed if the Lys surface motion were Brownian.[58] CTRW transport displays periods of immobility interrupted by desorption into the bulk punctuated by the adsorption to a new surface site. Single-frame displacement distributions quantify the hopping distances in the CTRW as Lys molecules travel to new sites on PS (Figure 2B). Single-frame displacement distributions show a clear dependence on the MW of the underlying PS film (Figure 2B). The decrease in hopping distances as MW is increased indicates that the mobility of Lys at PS is highly dependent on the chain structure of PS. We suggest that the packing of the PS chains (Table S1), discussed in the context of free volumes, has a direct impact on the distance between available adsorption sites on PS for Lys adsorption to occur (Scheme 1 in Supporting Information). The thicknesses of resulting PS films are quantified as a function of MW (Table S1), which shows that film thickness does not increase from 3k to 36k. An increase in film thickness is observed for the 1500k MW; however, we conclude that film thickness may not play a major role in protein dynamics PS surfaces given no thickness change is observed from 3k to 36k accompanied by a decrease in Lys mobility (Figure 2B). It must be noted that at the highest MW condition Lys is still highly mobile in comparison to α-LA, as shown in Figure 2B (black). In addition to the frame to frame displacements, hopping behavior is also quantified at the PS interfaces with varied MW.

Lys explores fewer adsorption sites at high MW PS with no change in the overall surface residence time, driven by an increase in waiting times at each adsorption site. The number of hops per trajectory is quantified in Figure 2C using the previously described filtering process,[43] where a hop is defined as a frame-to-frame displacement greater than our spatial resolution of 20 nm. Fewer hops per trajectory are observed in Figure 2C with increasing MW, indicating that Lys is less likely to readsorb to PS after desorption at higher MWs. Interestingly, the total surface residence time of Lys (Figure 2D) and the extracted desorption rate constants (Table S3) do

https://dx.doi.org/10.1021/acs.langmuir.9b03535
Langmuir 2020, 36, 2330−2338

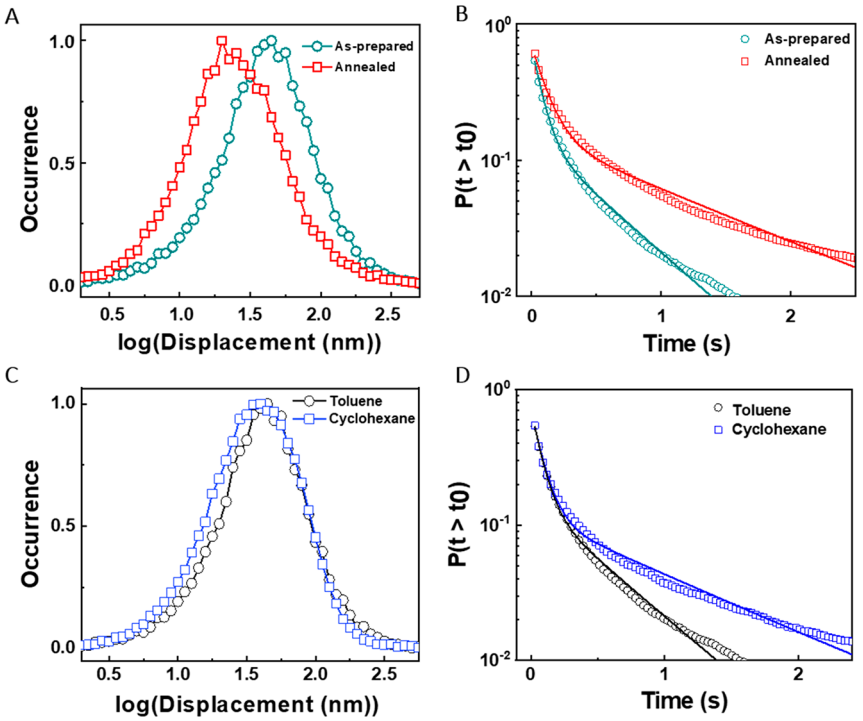

Figure 3. Lys dynamics at thermally annealed and cyclohexane-developed PS films with the molecular weight held constant at 36k for all conditions. (A) Single-frame displacement distributions for as-prepared and thermally annealed PS films. (B) Surface residence time distributions for as-prepared and thermally annealed PS films with fit to eq 1 shown with solid lines. (C) Single-frame displacement distributions for toluene- and cyclohexane-developed PS (MW = 36k). (D) Surface residence time distributions for toluene- and cyclohexane-developed PS films (MW = 36k) with fits to eq 1 shown with solid lines.

not change as a function of MW. Waiting time analyses show that as the MW is increased Lys spends more time per site before desorbing to a nearby site (Figure S6). Power law fits of waiting time distributions result in exponents of -2.02 ± 0.01, -1.84 ± 0.02, and -1.71 ± 0.02 for MWs of 3k, 36k, and 1500k, respectively (Figure S6). Although, Lys interacts with fewer adsorption sites during the CTRW as MW increases (Figure 2C), Lys spends more time at each site (Figure S6), accounting for the same total residence times for Lys at all MWs (Figure 2D). Single-molecule tracking allows for mechanistic details in the Lys CTRW to be related to the underlying free volumes in the PS films. To further confirm the impact of polymer free volume on the CTRW exhibited by Lys, two well-known methods, thermal annealing and adjusting solvent quality, are utilized to vary PS free volumes.

Lys Adsorption at Annealed and Cyclohexane-Developed PS Films. Lys dynamics at annealed PS show decreased single-frame displacements accompanied by increased surface residence times (Figure 3A, B). Thermally annealing PS films results in decreased free volumes through chain relaxation,[79] similar to increased MWs discussed above. Annealing allows us to further establish the relationship between PS free volumes and varied Lys CTRW dynamics. The annealing process is performed in inert nitrogen in order to minimize any chemical modifications to PS, but these effects cannot be completely ruled out. A shift in the single-frame displacement distributions is observed from peak values at 44 and 20 nm for as-prepared (MW = 36k) and thermally annealed PS films, respectively (Figure 3A, MW = 36k). The shift in single-frame hopping distances indicates that as PS chains pack more densely, Lys travels shorter distances to readsorb to the surface. The decrease in displacements with annealing (Figure 3A) is similar to the decrease observed with increased MW (Figure 2B), where decreased free volume leads to smaller displacements (Figure 2B). Annealing and MW displacement distributions confirm the hypothesis that as PS chains are packed more densely (Table S1), the distance between adsorption sites decreases, thereby leading to shorter displacements. Lys surface residence time increased as a result of thermally annealing PS (Figure 3B, Table S4). The increase in total Lys residence time with annealing (Figure 3B) is not observed in the case of increased MWs (Figure 2B). Annealing PS could induce different surface morphologies;[80] however, no statistical difference in surface roughness is found between the as-prepared and annealed PS surfaces (Figure S7). One likely explanation for observed increases in residence times on the annealed PS is the result of a greater reduction in PS free volume with annealing in comparison to increased MW (Figure 2), thereby leading to more short-range interactions between Lys and PS (Scheme 1 Supporting Information). This hypothesis is supported by the more severe shift in displacements observed at annealed PS centered at 20 nm (Figure 3A) in comparison to 39 nm in the highest MW condition (Figure 2B). Additionally the largest refractive index was measured for the annealed PS films, confirming the greatest increase in chain density, which can be related to decreased free volumes in thin films.[81] Minimal film thickness changes were observed as a result of annealing. To further support the structure−function relationship in PS free volume to Lys CTRW dynamics, a poor solvent is investigated for the development of PS films.

Decreased Lys hopping distances are observed on the PS films developed in a poor solvent in addition to an increased surface residence time, aligning with the observations seen in

https://dx.doi.org/10.1021/acs.langmuir.9b03535
Langmuir 2020, 36, 2330−2338

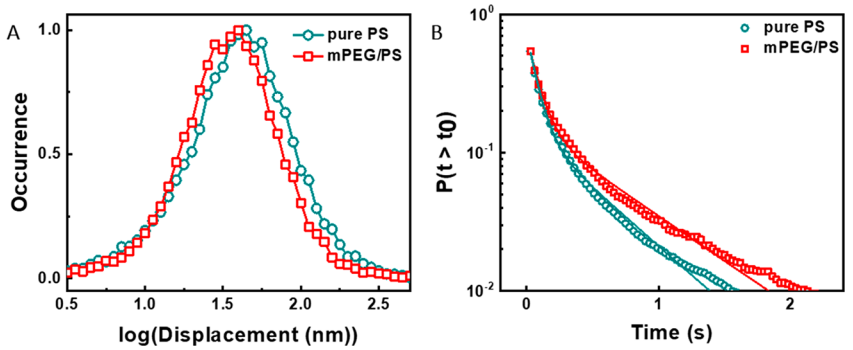

Figure 4. Comparison of Lys dynamics at as-prepared and mPEG-doped PS films with the molecular weight held constant at 36k for all conditions. (A) The distributions of single-frame displacements at as-prepared and mPEG-doped PS films (MW = 36k). (D) Cumulative distribution of surface residence time for Lys adsorption at as-prepared and mPEG-doped PS films (MW = 36k). Solid lines are fits to eq 1.

the annealing conditions. Decreasing solvent quality to decrease polymer chain free volumes is well studied, in particular using cyclohexane to develop PS films.[82,83] Decreased free volumes in resulting PS films using a poor solvent is driven by decreased PS solubility in the cyclohexane. A decrease in hopping distances from a peak maximum at 44 to 39 nm is observed from the toluene (MW = 36k) to cyclohexane-deposited PS, respectively (Figure 3C, MW = 36k). Our observations of Lys surface dynamics establish that the distance between adsorption sites for Lys is dictated by the size of free volumes present in a PS film. The change observed for single-frame displacements with cyclohexane-deposited PS is the same magnitude observed in the case of varied MW (Figure 2B). However, we observe an increase in residence time of Lys as the PS chain density is increased (Figure 3D, Table S5) similar to that observed on the thermally annealed PS (Figure 3B, Table S4). We predict the increased residence time is driven by an increased number of short-range interactions between the PS chains and Lys. To further develop the mechanistic understanding of hindered CTRW dynamics exhibited by Lys at PS, the dominant short-range interaction driving hindered CTRW dynamics is investigated next.

Driving Forces of Lys Dynamics at PS. Tracking results under altered solution and PS film chemistries suggest that hydrophobic effects, rather than electrostatic effects, are the primary driver of the hindered CTRW dynamics at PS. The contributions of electrostatics in our observed dynamics are tested with the addition of 20 and 100 mM NaCl during Lys tracking at the PS interface (Figure S8). Although PS chains carry no charge,[46] Lys carries a net positive charge at our experimental conditions (pH = 7.2), and the presence of PS impurities could not be ruled out. Single-frame displacement results indicate that electrostatics are not the dominant driving force in the observed CTRW Lys dynamics (Figure S8). To evaluate the effect of hydrophobic interactions, PS (MW = 36k) is doped with 10 w/w% mPEG to increase the hydrophilicity of the PS film.[84] AFM imaging results indicate that mPEG domains are highly uniform within the PS films (Figure S1). Single-frame displacement distributions show a decrease from 44 to 39 nm as the surface becomes more hydrophilic with mPEG doping (Figure 4A). If long-range hopping does exist as a result of large isolated mPEG domains, it would not be detected given diffusion in the bulk would be faster than our detectors temporal resolution and/or outside of the evanescent field present in our TIRF illumination geometry.[71] An increase in surface residence time is observed on the more hydrophilic doped PS film (Figure 4B, Table S6). Single-frame distributions and residence time distribution changes with mPEG doping align well with observed Lys dynamics as a function of MW, thermal annealing, and solvent at the PS surfaces. Therefore, we suggest hydrophobics to be the dominating force in the interactions of Lys at PS. Our previous study of Lys at functionalized PS interfaces also reveals that hydrophobics dominate hindered Lys CTRW dynamics as PS becomes more hydrophilic.[17] Previous work shows that hydrophobics can also play a large role in 3D transport dynamics in porous media.[85] Here, a more careful look at single protein tracking results suggests that the underlying microstructure of PS yields similar effects without the introduction of new charge carrying chemistries to PS.[17] Although similar results and driving forces are at play in both cases, here we uncover a structure−function relationship present in Lys dynamics at PS without modifying the overall hydrophobicity of the thin PS film (Figures 1−3). It must be noted that contributions from van der Waals forces, changes in free volumes from mPEG doping, and hydrogen bonding cannot be ruled out as contributors as well. However, based on our single-molecule observables, van der Waals forces and hydrogen bonding are likely minor contributors based on the decrease in hopping distances and the increase in residence times, which align with observables from MW, annealing, and solvent quality.

CONCLUSION

Here, single-molecule tracking and superlocalization microscopy are used to establish a relationship between the underlying PS free volume to the dynamics of two proteins α-LA and Lys. Super-resolution imaging, along with the single-molecule tracking, verify that α-LA molecules are immobilized at nonspecific adsorption sites with increased residence times as PS free volumes decrease as a function of PS MWs. Although Lys is similar in size and structure to α-LA, Lys molecules exhibit a CTRW at PS. The mechanism of Lys CTRW transport, hopping dynamics, and single-site waiting times are dependent on the underlying MW of PS. We propose the varied CTRW dynamics exhibited by Lys are likely caused by the variation in PS free volumes in the films with different MWs. This hypothesis is further supported by decreasing PS free volumes with thermal annealing and adjusting solvent quality, both resulting in smaller free volumes and increased PS chain packing. Displacement distributions at the annealed and solvent-modified PS corroborate the relationship between

https://dx.doi.org/10.1021/acs.langmuir.9b03535
Langmuir 2020, 36, 2330−2338

hindered CTRW dynamics and decreased PS free volumes. Longer residence times were observed for Lys at the annealed and decreased solvent quality PS attributed to more severe reductions in PS free volumes in comparison to varied MW, thereby introducing more short-range interactions between Lys and PS. Lastly, the dominant force driving hindered CTRW dynamics at PS as the free volumes decreased is interpretted to be hydrophobics with minimal contributions from electrostatic forces. The distinct dynamics exhibited by two structurally and biologically related model proteins on chemically identical surfaces illustrate the complexity in protein−polymer interactions. More specifically we highlight the relation between underlying free volumes in a commonly utilized polymer film, PS, to nanoscale protein transport dynamics. Our findings here can have broad impacts on the design of application-specific polymer materials[4] where suppressing anomalous surface diffusion would be advantageous for decreasing the prevalence of protein unfolding and denaturation at strong adsorption sites[47] and improving protein separation efficiencies.[43]

■ ASSOCIATED CONTENT

Supporting Information

The Supporting Information is available free of charge at https://pubs.acs.org/doi/10.1021/acs.langmuir.9b03535.

Polystyrene film thicknesses and refractive indices, CTRW vs chain density scheme, AFM imaging of mPEG-doped polystyrene films, dye structures, TIRF setup and representative α-lactalbumin image, α-lactalbumin and lysozyme structures, lysozyme residence time with varied dye labels, α-lactalbumin surface residence time fit results, lysoszyme waiting time analyses and power law fitting results, lysozyme surface residence time fit results at molecular weight varied polystyrene, lysozyme surface residence time fit results at annealed polystyrene, lysozyme surface residence time fit results at solvent varied polystrene, AFM imaging of PS before and after annealing, single-frame displacement distrubtions under varied salt conditions, and lysozyme surface residence time fit results at mPEG-doped polystyrene (PDF)

■ AUTHOR INFORMATION

Corresponding Author

Christy F. Landes − *Department of Chemistry, Department of Electrical and Computer Engineering, Department of Chemical and Biomolecular Engineering, and Smalley-Curl Institute, Rice University, Houston, Texas 77251, United States;* orcid.org/0000-0003-4163-6497; Email: cflandes@rice.edu

Authors

Nicholas A. Moringo − *Department of Chemistry, Rice University, Houston, Texas 77251, United States;* orcid.org/0000-0002-0044-255X

Hao Shen − *Department of Chemistry, Rice University, Houston, Texas 77251, United States;* orcid.org/0000-0002-2798-5861

Lawrence J. Tauzin − *Department of Chemistry, Rice University, Houston, Texas 77251, United States;* orcid.org/0000-0003-3254-1533

Wenxiao Wang − *Department of Electrical and Computer Engineering, Rice University, Houston, Texas 77251, United States*

Complete contact information is available at: https://pubs.acs.org/10.1021/acs.langmuir.9b03535

Author Contributions

#These uthors equally contributed to the presented work.

Notes

The authors declare no competing financial interest.

■ ACKNOWLEDGMENTS

This research is supported by the NSF (CHE-1808382) and the Welch Foundation (C-1787). N.A.M. acknowledges that this material is based upon work supported by the National Science Foundation Graduate Research Fellowship Program (1842494). We thank the Wilson research group at the University of Houston for previsouly providing the labeled α-LA, and the Link group at Rice University for discussions. Ellipsometry and atomic force microscopy measurements were performed using the facilities of the Shared Equipment Authority at Rice University.

■ REFERENCES

(1) Hahm, J. I. Fundamentals of Nanoscale Polymer-Protein Interactions and Potential Contributions to Solid-State Nanobioarrays. *Langmuir* **2014**, *30*, 9891−9904.

(2) Song, S.; Ravensbergen, K.; Alabanza, A.; Soldin, D.; Hahm, J.-i. Distinct Adsorption Configurations and Self-Assembly Characteristics of Fibrinogen on Chemically Uniform and Alternating Surfaces including Block Copolymer Nanodomains. *ACS Nano* **2014**, *8*, 5257−5269.

(3) Wang, Z.; Yan, Y.; Qiao, L. Protein adsorption on implant metals with various deformed surfaces. *Colloids Surf., B* **2017**, *156*, 62−70.

(4) Wei, Q.; Becherer, T.; Angioletti-Uberti, S.; Dzubiella, J.; Wischke, C.; Neffe, A. T.; Lendlein, A.; Ballauff, M.; Haag, R. Protein interactions with polymer coatings and biomaterials. *Angew. Chem., Int. Ed.* **2014**, *53*, 8004−31.

(5) Moringo, N. A.; Shen, H.; Bishop, L. D.; Wang, W.; Landes, C. F. Enhancing Analytical Separations Using Super-Resolution Microscopy. *Annu. Rev. Phys. Chem.* **2018**, *69*, 353−375.

(6) Kisley, L.; Chen, J.; Mansur, A. P.; Shuang, B.; Kourentzi, K.; Poongavanam, M. V.; Chen, W. H.; Dhamane, S.; Willson, R. C.; Landes, C. F. Unified superresolution experiments and stochastic theory provide mechanistic insight into protein ion-exchange adsorptive separations. *Proc. Natl. Acad. Sci. U. S. A.* **2014**, *111*, 2075−80.

(7) Yu, C.; Granick, S. Revisiting Polymer Surface Diffusion in the Extreme Case of Strong Adsorption. *Langmuir* **2014**, *30*, 14538−14544.

(8) Michael, K. E.; Vernekar, V. N.; Keselowsky, B. G.; Meredith, J. C.; Latour, R. A.; García, A. J. Adsorption-Induced Conformational Changes in Fibronectin Due to Interactions with Well-Defined Surface Chemistries. *Langmuir* **2003**, *19*, 8033−8040.

(9) Hu, W.-J.; Eaton, J. W.; Ugarova, T. P.; Tang, L. Molecular basis of biomaterial-mediated foreign body reactions. *Blood* **2001**, *98*, 1231−1238.

(10) Garrett, Q.; Garrett, R. W.; Milthorpe, B. K. Lysozyme sorption in hydrogel contact lenses. *Investigative Ophthalmology & Visual Science* **1999**, *40*, 897−903.

(11) Deng, X. M.; Castillo, E. J.; Anderson, J. M. Surface modification of soft contact lenses: Silanization, wettability and lysozyme adsorption studies. *Biomaterials* **1986**, *7*, 247−251.

(12) Nabe, A.; Staude, E.; Belfort, G. Surface modification of polysulfone ultrafiltration membranes and fouling by BSA solutions. *J. Membr. Sci.* **1997**, *133*, 57−72.

(13) Daniels, C. R.; Reznik, C.; Kilmer, R.; Felipe, M. J.; Tria, M. C. R.; Kourentzi, K.; Chen, W. H.; Advincula, R. C.; Willson, R. C.; Landes, C. F. Permeability of anti-fouling PEGylated surfaces probed

by fluorescence correlation spectroscopy. *Colloids Surf., B* **2011**, *88*, 31−38.
(14) Zhang, D.; Dougal, S.; Yeganeh, M. Effects of UV irradiation and plasma treatment on a polystyrene surface studied by IR-visible sum frequency generation spectroscopy. *Langmuir* **2000**, *16*, 4528−4532.
(15) Szleifer, I. Protein adsorption on tethered polymer layers: effect of polymer chain architecture and composition. *Phys. A* **1997**, *244*, 370−388.
(16) Herrwerth, S.; Eck, W.; Reinhardt, S.; Grunze, M. Factors that determine the protein resistance of oligoether self-assembled monolayers- internal hydrophilicity, terminal hydrophilicity, and lateral packing density. *J. Am. Chem. Soc.* **2003**, *125*, 9359−9366.
(17) Moringo, N. A.; Shen, H.; Tauzin, L. J.; Wang, W.; Bishop, L. D.; Landes, C. F. Variable lysozyme transport dynamics on oxidatively functionalized polystyrene films. *Langmuir* **2017**, *33*, 10818−10828.
(18) Yu, Z.; Yahsi, U.; McGervey, J.; Jamieson, A.; Simha, R. Molecular weight-dependence of free volume in polystyrene studied by positron annihilation measurements. *J. Polym. Sci., Part B: Polym. Phys.* **1994**, *32*, 2637−2644.
(19) White, R. P.; Lipson, J. E. Polymer free volume and its connection to the glass transition. *Macromolecules* **2016**, *49*, 3987−4007.
(20) Tant, M.; Wilkes, G. An overview of the nonequilibrium behavior of polymer glasses. *Polym. Eng. Sci.* **1981**, *21*, 874−895.
(21) Nagel, C.; Günther-Schade, K.; Fritsch, D.; Strunskus, T.; Faupel, F. Free volume and transport properties in highly selective polymer membranes. *Macromolecules* **2002**, *35*, 2071−2077.
(22) Kobayashi, Y.; Zheng, W.; Meyer, E.; McGervey, J.; Jamieson, A.; Simha, R. Free volume and physical aging of poly (vinyl acetate) studied by positron annihilation. *Macromolecules* **1989**, *22*, 2302−2306.
(23) Malekmotiei, L.; Voyiadjis, G. Z.; Samadi-Dooki, A.; Lu, F.; Zhou, J. Effect of annealing temperature on interrelation between the microstructural evolution and plastic deformation in polymers. *J. Polym. Sci., Part B: Polym. Phys.* **2017**, *55*, 1286−1297.
(24) Cho, N.-J.; Frank, C. W.; Kasemo, B.; Höök, F. Quartz crystal microbalance with dissipation monitoring of supported lipid bilayers on various substrates. *Nat. Protoc.* **2010**, *5*, 1096−1106.
(25) Liu, M.; Zhang, Y.; Wang, M.; Deng, C.; Xie, Q.; Yao, S. Adsorption of bovine serum albumin and fibrinogen on hydrophilicity-controllable surfaces of polypyrrole doped with dodecyl benzene sulfonate—A combined piezoelectric quartz crystal impedance and electrochemical impedance study. *Polymer* **2006**, *47*, 3372−3381.
(26) Pothula, K. R.; Smyrnova, D.; Schröder, G. F. Clustering cryo-EM images of helical protein polymers for helical reconstructions. *Ultramicroscopy* **2019**, *203*, 132−138.
(27) Song, S.; Xie, T.; Ravensbergen, K.; Hahm, J. I. Ascertaining effects of nanoscale polymeric interfaces on competitive protein adsorption at the individual protein level. *Nanoscale* **2016**, *8*, 3496−509.
(28) Shen, H.; Tauzin, L. J.; Wang, W.; Hoener, B.; Shuang, B.; Kisley, L.; Hoggard, A.; Landes, C. F. Single-Molecule Kinetics of Protein Adsorption on Thin Nylon-6, 6 Films. *Anal. Chem.* **2016**, *88*, 9926−9933.
(29) Lord, S. J.; Lee, H.-l. D.; Moerner, W. Single-molecule spectroscopy and imaging of biomolecules in living cells. *Anal. Chem.* **2010**, *82*, 2192−2203.
(30) Wirth, M. J.; Swinton, D. J. Single-molecule probing of mixed-mode adsorption at a chromatographic interface. *Anal. Chem.* **1998**, *70*, 5264−5271.
(31) Faulón Marruecos, D.; Kastantin, M.; Schwartz, D. K.; Kaar, J. L. Dense Poly (ethylene glycol) Brushes Reduce Adsorption and Stabilize the Unfolded Conformation of Fibronectin. *Biomacromolecules* **2016**, *17*, 1017−1025.
(32) Daniels, C. R.; Tauzin, L. J.; Foster, E.; Advincula, R. C.; Landes, C. F. On the pH-Responsive, Charge-Selective, Polymer-Brush-Mediated Transport Probed by Traditional and Scanning Fluorescence Correlation Spectroscopy. *J. Phys. Chem. B* **2013**, *117*, 4284−4290.
(33) Chin, H.-Y.; Wang, D.; Schwartz, D. K. Dynamic Molecular Behavior on Thermoresponsive Polymer Brushes. *Macromolecules* **2015**, *48*, 4562−4571.
(34) Tauzin, L. J.; Shuang, B.; Kisley, L.; Mansur, A. P.; Chen, J.; de Leon, A.; Advincula, R. C.; Landes, C. F. Charge-Dependent Transport Switching of Single Molecular Ions in a Weak Polyelectrolyte Multilayer. *Langmuir* **2014**, *30*, 8391−8399.
(35) Giri, D.; Ashraf, K. M.; Collinson, M. M.; Higgins, D. A. Single-Molecule Perspective on Mass Transport in Condensed Water Layers over Gradient Self-Assembled Monolayers. *J. Phys. Chem. C* **2015**, *119*, 9418−9428.
(36) Wang, W.; Shen, H.; Shuang, B.; Hoener, B. S.; Tauzin, L. J.; Moringo, N. A.; Kelly, K. F.; Landes, C. F. Super Temporal-Resolved Microscopy (STReM). *J. Phys. Chem. Lett.* **2016**, *7*, 4524.
(37) Cooper, J. T.; Peterson, E. M.; Harris, J. M. Fluorescence Imaging of Single-Molecule Retention Trajectories in Reversed-Phase Chromatographic Particles. *Anal. Chem.* **2013**, *85*, 9363−9370.
(38) Shen, H.; Zhou, X.; Zou, N.; Chen, P. Single-molecule kinetics reveals a hidden surface reaction intermediate in single-nanoparticle catalysis. *J. Phys. Chem. C* **2014**, *118*, 26902−26911.
(39) Shen, H.; Xu, W.; Chen, P. Single-molecule nanoscale electrocatalysis. *Phys. Chem. Chem. Phys.* **2010**, *12*, 6555−6563.
(40) Cordes, T.; Moerner, W.; Orrit, M.; Sekatskii, S.; Faez, S.; Borri, P.; Prabal Goswami, H.; Clark, A.; El-Khoury, P.; Mayr, S.; et al. Plasmonics, tracking and manipulating, and living cells: general discussion. *Faraday Discuss.* **2015**, *184*, 451−473.
(41) Shen, H.; Tauzin, L. J.; Baiyasi, R.; Wang, W.; Moringo, N.; Shuang, B.; Landes, C. F. Single Particle Tracking: From Theory to Biophysical Applications. *Chem. Rev.* **2017**, *117*, 7331.
(42) Bishop, L. D.; Landes, C. F. From a Protein's Perspective: Elution at the Single-Molecule Level. *Acc. Chem. Res.* **2018**, *51*, 2247−2254.
(43) Moringo, N. A.; Bishop, L. D. C.; Shen, H.; Misiura, A.; Carrejo, N. C.; Baiyasi, R.; Wang, W.; Ye, F.; Robinson, J. T.; Landes, C. F. A mechanistic examination of salting out in protein-polymer membrane interactions. *Proc. Natl. Acad. Sci. U. S. A.* **2019**, *116*, 22938.
(44) Huopalahti, R.; Anton, M.; López-Fandiño, R.; Schade, R. *Bioactive Egg Compounds*; Springer: 2007.
(45) Bramaud, C.; Aimar, P.; Daufin, G. Whey protein fractionation: Isoelectric precipitation of α-lactalbumin under gentle heat treatment. *Biotechnol. Bioeng.* **1997**, *56*, 391−397.
(46) Breite, D.; Went, M.; Prager, A.; Schulze, A. Tailoring membrane surface charges: A novel study on electrostatic interactions during membrane fouling. *Polymers* **2015**, *7*, 2017−2030.
(47) Weltz, J. S.; Schwartz, D. K.; Kaar, J. L. Surface-Mediated Protein Unfolding as a Search Process for Denaturing Sites. *ACS Nano* **2016**, *10*, 730−738.
(48) Swaminathan, R.; Ravi, V. K.; Kumar, S.; Kumar, M. V. S.; Chandra, N. Lysozyme: a model protein for amyloid research. In *Advances in Protein Chemistry and Structural Biology*; Elsevier: 2011; Vol. *84*, pp 63−111.
(49) Permyakov, E. A.; Berliner, L. J. α-Lactalbumin: structure and function. *FEBS Lett.* **2000**, *473*, 269−274.
(50) Ulusan, S.; Bütün, V.; Banerjee, S.; Erel-Goktepe, I. Biologically Functional Ultrathin Films Made of Zwitterionic Block Copolymer Micelles. *Langmuir* **2019**, *35*, 1156−1171.
(51) Wang, W.; Shen, H.; Moringo, N. A.; Carrejo, N. C.; Ye, F.; Robinson, J. T.; Landes, C. F. Super-temporal resolved microscopy reveals multistep desorption kinetics of α-lactalbumin from nylon. *Langmuir* **2018**, *34*, 6697−6702.
(52) Iyer, L. K.; Qasba, P. K. Molecular dynamics simulation of α-lactalbumin and calcium binding c-type lysozyme. *Protein Eng., Des. Sel.* **1999**, *12*, 129−139.
(53) Acharya, K. R.; Stuart, D. I.; Walker, N. P. C.; Lewis, M.; Phillips, D. C. Refined structure of baboon α-lactalbumin at 1.7 Å

https://dx.doi.org/10.1021/acs.langmuir.9b03535
Langmuir 2020, 36, 2330−2338

resolution: Comparison with C-type lysozyme. *J. Mol. Biol.* **1989**, *208*, 99−127.
(54) Teare, D.; Emmison, N.; Ton-That, C.; Bradley, R. Cellular attachment to ultraviolet ozone modified polystyrene surfaces. *Langmuir* **2000**, *16*, 2818−2824.
(55) Feng, Y.; Borrelli, M.; Meyer-ter-Vehn, T.; Reichl, S.; Schrader, S.; Geerling, G. Epithelial wound healing on keratin film, amniotic membrane and polystyrene in vitro. *Curr. Eye Res.* **2014**, *39*, 561−570.
(56) Bekele, S.; Tsige, M. Interfacial properties of oxidized polystyrene and its interaction with water. *Langmuir* **2013**, *29*, 13230−13238.
(57) Honciuc, A.; Harant, A. W.; Schwartz, D. K. Single-molecule observations of surfactant diffusion at the solution- solid interface. *Langmuir* **2008**, *24*, 6562−6566.
(58) Walder, R.; Nelson, N.; Schwartz, D. K. Single molecule observations of desorption-mediated diffusion at the solid-liquid interface. *Phys. Rev. Lett.* **2011**, *107*, 156102.
(59) McUmber, A. C.; Randolph, T. W.; Schwartz, D. K. Electrostatic interactions influence protein adsorption (but not desorption) at the silica-aqueous interface. *J. Phys. Chem. Lett.* **2015**, *6*, 2583−2587.
(60) Parmar, A. S.; Muschol, M. Hydration and hydrodynamic interactions of lysozyme: effects of chaotropic versus kosmotropic ions. *Biophys. J.* **2009**, *97*, 590−598.
(61) Gast, K.; Zirwer, D.; MÜller-Frohne, M.; Damaschun, G. Compactness of the kinetic molten globule of bovineα-lactalbumin: A dynamic light scattering study. *Protein Sci.* **1998**, *7*, 2004−2011.
(62) Ma, X.; Lu, J. Q; Brock, R S.; Jacobs, K. M; Yang, P.; Hu, X.-H. Determination of complex refractive index of polystyrene microspheres from 370 to 1610 nm. *Phys. Med. Biol.* **2003**, *48*, 4165.
(63) Shuang, B.; Chen, J.; Kisley, L.; Landes, C. F. Troika of single particle tracking programing: SNR enhancement, particle identification, and mapping. *Phys. Chem. Chem. Phys.* **2014**, *16*, 624−634.
(64) Langdon, B. B.; Mirhossaini, R. B.; Mabry, J. N.; Sriram, I.; Lajmi, A.; Zhang, Y. X.; Rojas, O. J.; Schwartz, D. K. Single-Molecule Resolution of Protein Dynamics on Polymeric Membrane Surfaces: The Roles of Spatial and Population Heterogeneity. *ACS Appl. Mater. Interfaces* **2015**, *7*, 3607−3617.
(65) Bates, M.; Huang, B.; Dempsey, G. T.; Zhuang, X. Multicolor Super-Resolution Imaging with Photo-Switchable Fluorescent Probes. *Science* **2007**, *317*, 1749−1753.
(66) Xu, W.; Shen, H.; Kim, Y. J.; Zhou, X.; Liu, G.; Park, J.; Chen, P. Single-Molecule Electrocatalysis by Single-Walled Carbon Nanotubes. *Nano Lett.* **2009**, *9*, 3968−3973.
(67) Betzig, E.; Patterson, G. H.; Sougrat, R.; Lindwasser, O. W.; Olenych, S.; Bonifacino, J. S.; Davidson, M. W.; Lippincott-Schwartz, J.; Hess, H. F. Imaging Intracellular Fluorescent Proteins at Nanometer Resolution. *Science* **2006**, *313*, 1642−1645.
(68) Rust, M. J.; Bates, M.; Zhuang, X. Sub-diffraction-limit imaging by stochastic optical reconstruction microscopy (STORM). *Nat. Methods* **2006**, *3*, 793−796.
(69) Chen, J.; Bremauntz, A.; Kisley, L.; Shuang, B.; Landes, C. F. Super-Resolution mbPAINT for Optical Localization of Single-Stranded DNA. *ACS Appl. Mater. Interfaces* **2013**, *5*, 9338−9343.
(70) Peterson, E. M.; Manhart, M. W.; Harris, J. M. Competitive Assays of Label-Free DNA Hybridization with Single-Molecule Fluorescence Imaging Detection. *Anal. Chem.* **2016**, *88*, 6410−6417.
(71) Peterson, E. M.; Manhart, M. W.; Harris, J. M. Single-Molecule Fluorescence Imaging of Interfacial DNA Hybridization Kinetics at Selective Capture Surfaces. *Anal. Chem.* **2016**, *88*, 1345−1354.
(72) James, S.; McManus, J. J. Thermal and solution stability of lysozyme in the presence of sucrose, glucose, and trehalose. *J. Phys. Chem. B* **2012**, *116*, 10182−10188.
(73) West, D.; McBrierty, V.; Delaney, C. Positron decay in polymers: Molecular weight dependence in polystyrene. *Appl. Phys.* **1975**, *7*, 171−174.
(74) Montroll, E. W.; Weiss, G. H. Random walks on lattices. II. *J. Math. Phys.* **1965**, *6*, 167−181.
(75) Nitta, K.; Sugai, S. The evolution of lysozyme and α-lactalbumin. *Eur. J. Biochem.* **1989**, *182*, 111−118.
(76) Nitta, K. α-Lactalbumin and (Calcium-Binding) Lysozyme. In *Calcium-Binding Protein Protocols*; Vogel, H., Ed.; Humana Press: 2002; Vol. *172*, pp 211−224.
(77) Qasba, P. K.; Kumar, S.; Brew, K. Molecular Divergence of Lysozymes and α-Lactalbumin. *Crit. Rev. Biochem. Mol. Biol.* **1997**, *32*, 255−306.
(78) Skaug, M. J.; Mabry, J.; Schwartz, D. K. Intermittent Molecular Hopping at the Solid-Liquid Interface. *Phys. Rev. Lett.* **2013**, *110*, 256101.
(79) Sandreczki, T.; Hong, X.; Jean, Y. Sub-glass-transition-temperature annealing of polycarbonate studied by positron annihilation spectroscopy. *Macromolecules* **1996**, *29*, 4015−4018.
(80) Ton-That, C.; Shard, A.; Daley, R.; Bradley, R. Effects of annealing on the surface composition and morphology of PS/PMMA blend. *Macromolecules* **2000**, *33*, 8453−8459.
(81) Hougham, G.; Tesoro, G.; Viehbeck, A. Influence of free volume change on the relative permittivity and refractive index in fluoropolyimides. *Macromolecules* **1996**, *29*, 3453−3456.
(82) Sugiyama, M.; Nakamura, Y.; Norisuye, T. Dilute-solution properties of polystyrene polymacromonomer having side chains of over 100 monomeric units. *Polym. J.* **2008**, *40*, 109.
(83) Wang, R.; Wang, Z.-G. Theory of polymer chains in poor solvent: Single-chain structure, solution thermodynamics, and θ point. *Macromolecules* **2014**, *47*, 4094−4102.
(84) Ayen, W. Y.; Chintankumar, B.; Jain, J. P.; Kumar, N. Effect of PEG chain length and hydrophilic weight fraction on polymersomes prepared from branched (PEG) 3-PLA co-polymers. *Polym. Adv. Technol.* **2011**, *22*, 158−165.
(85) Brumaru, C.; Geng, M. L. Interaction of surfactants with hydrophobic surfaces in nanopores. *Langmuir* **2010**, *26*, 19091−19099.

https://dx.doi.org/10.1021/acs.langmuir.9b03535
Langmuir 2020, 36, 2330−2338